IJESRT: 12(5), May, 2023 ISSN: 2277-9655

International Journal of Engineering Sciences & Research Technology

(A Peer Reviewed Online Journal)
Impact Factor: 5.164

IJESRT

Website: www.ijesrt.com Mail: editor@ijesrt.com

Correspondence Address: 116, Sukhdev Nagar Ext-1, Airport Road, Indore – 452005, Madhya Pradesh, INDIA

ISSN: 2277-9655
Impact Factor: 5.164
CODEN: IJESS7

IJESRT

INTERNATIONAL JOURNAL OF ENGINEERING SCIENCES & RESEARCH TECHNOLOGY

DETERMINATION OF CURRENT DENSITY AND RECOMBINATION RATE OF BORON DOPED BACKGROUND AND PHOSPHORUS DOPED EMITTER SILICON SOLAR CELL UNDER MONOCHROMATIC ILLUMINATION.

Papa Touty Traore[*1], **Modou Pilor, Mor Ndiaye, and Issa Diagne**
[*] Department of physics, Cheikh Anta Diop University, Senegal

DOI: Will get Assigned by IJESRT Team

ABSTRACT

The aim of the work is to determine the recombination in a heavily doped region of silicon, such as an emitter. The emitter saturation current density is also determined in this work. The model set-up an emitter's surface recombination velocity from an experimentally measured J0E.Also both types are considered such that, the radiative and the auger. The SHR recombination is applied in the emitter. The dopand species is the phosphorus in the emitter and the boron in the background. The recombination rate and the current density are obtained under the monochromatic light illumination and the outdoor temperature.

KEYWORDS: current density-recombination-emitter-silicon -solar cell.

1. INTRODUCTION

The simulation of heavily doped silicon [1] is a contentious field. Models for Auger recombination [2] , carrier mobility [3], and especially bandgap narrowing, have not been validated over a wide range of experimental dopant profiles, primarily because these fundamental properties are difficult to measure in heavily doped silicon [4] . Since in typical silicon solar cells [5], the dopant profile of the emitter (or back-surface field) decreases below the background dopant concentration [6], it might seem like its boundary could be defined as the location where the two concentrations are equal. This point is called the metallurgical junction [7]. Yet at equilibrium, and many conditions besides, a depletion region exists at the metallurgical junction that cannot be considered a part of an emitter. (The quasi-neutral assumption does not hold in a depletion region.) EDNA 2 [8] software permits the user to define the boundary of the emitter. The boundary is only important when Shockley–Read–Hall (SRH) recombination in the emitter is significant. The calculation of the surface recombination rate is solved by the approach of Girisch et al. [9], which assumes that the quasi-Fermi levels are constant within the surface space-charge region. In this work the recombination rate in the heavily doped region in the current density are determined.

2. MATERIALS AND METHODS

Materials

The material set-up in this model is given by the tables below.

Table 1 Background parameters

Background	
Dopant species	Boron
Concentration N_b	10^{16}
Resistivity	1.46 Ω/sq

Table 2 Emitter parameters

Emitter	
Dopant species	Phosphorus
Profile	Generated
Sheet resistance	117 Ω/sq
Function	ERFC
N_{peak}	3.10^{19} cm^{-3}

Z_{peak}	0 um
Zf	0.3 um

Table 3 Recombination model

Recombination models	
Radiative	Fell2021
Auger	Niewelt 2022
SRH at surface	Sn0, sp0,Eit &Qf
Sn0	100000cm/s
Eit-Ei	0ev
Tno	100us
Et-Ei	0 ev
Spo	100000cm/s
Qf	0 cm^{-2}
TP0	100us

Table 4 Excitation parameters

Excitation	
Specific voltage $V_{j\ spec}$	0.55 V
Temperature	300 K

SHR Recombination in the emitter.
Table 5 Generation parameters

Generation	
Spectrum	Monochromatic
Wavelenght	300nm
Absorption coefficient	1.77 10^6 cm^{-1}

Table 6 Mobility and band gap models

Mobility and band gap models	
Mobility mdoel	Klaasen 1992
Intrinsic band gap	Passler 2002
Density of states	Sentaurus 2008 DOS Form.2
Doapnd ionisation	Altmatt 2006
Carrier statistics	Fermi-Dirac
Bnad gap norrowing	Schenk 1998

Table 7 Miscellaneous model

Miscellaneous	
Definition of Z_f	PC1D
Auger	Niewelt 2022
SRH at surface	Sn0, sp0,Eit &Qf

The effective depth of the emitter is defined as first point where either.
Condition 1 $n_0 = 10 \times N_b$
Condition 2 $n_0 = 1 \times \Delta N_b$
SHR Recombination model is applied in the emitter.

Methods

The EDNA 2 algorithm begins by loading the background and emitter dopant profiles and calculating the emitter's sheet resistance in equilibrium. An explanation of the functions used to generate the emitter profile, and the equations used to calculate the sheet resistance, are given.

EDNA 2 then computes the intrinsic and equilibrium parameters of the silicon as a function of depth. These parameters include the ionised donor ND+ and accetor NA– concentrations, the effective intrinsic carrier concentration ni eff, the conduction band energy Ec, the valence band energy Ev, the electron Fermi energy EFn, and the hole Fermi energy EFp, following the procedure used in the band gap calculator.

Next, the excess carrier density is set at the surface Δn(0), providing the first of two boundary conditions. EDNA 2 then computes the surface recombination and applies the shooting method to determine the excess carriers as a function of depth within the emitter. This requires the computation of the recombination rate,.

Once the excess carrier density is known as a function of depth, the effective width of the emitter is determined from two (somewhat arbitrary) conditions specified in the Options. When SRH recombination in the emitter is small, the exact effective width is unimportant because little recombination occurs deep in the emitter (since in this case, the total recombination is dominated by Auger recombination near the front surface). But when SRH recombination in the emitter is large, the definition of the emitter boundary is crucial, and it causes the total recombination to depend on the conditions used to define the lower boundary. This problem arises whenever attributing recombination to an emitter.

Having established the emitter's lower boundary, EDNA 2 calls this the 'junction'. A junction voltage Vj and a collection current Jj is then calculated from the carrier concentrations.

Finally, EDNA 2 iterates, varying Δn(0) and computing Vj and Jj, until one of four cases have been met (the second boundary condition). The first case is the dark case (when there is no generation) and when Vj equals the user-specified junction voltage. This gives a 'dark solution'. The other three cases relate to illuminated (or light) conditions, when a generation rate within the emitter is calculated from the generation inputs. EDNA 2 finds solutions for (i) the short-circuit case defined as Vj = 0, (ii) the open-circuit case defined as Jj = 0, and (iii) the case where Vj equals the specified junction voltage.

3 RESULTS AND DISCUSSION

The tables below show the outputs obtained after computing the model at short circuit, at open circuit and at specified voltage.

Table 8 Emitter major parameters

Emitter Sheet resistance at equilibrium	ρ_{sq}	117 Ω/sq
Emitter saturation current at 0.55 V	J_{OE}	69.6 fA/cm^2
Emitter collection efficiency at short circuit	IQE_E	93.5 %

Table 9 The effective emitter width and the junction voltage at different voltage

	At Short-circuit	At open circuit	At specified voltage
Eff emitter width (um)	0.617	0.617	0.617
Junction voltage	2.15 10^{-4}	0.698	0.550

The effective emitter width is constant at short circuit, open circuit, and specified voltage. The junction volage depends on whether the condition is short circuit, open circuit, or specified voltage. The outputs obtained shows that the junction volage is most important at open circuit compared to short circuit and specified voltage where the junction are respectively 2.15 10^{-4} V and 0.550 V.

Table 10 The current density at different voltage

Currents (mA/cm^2)	At Short-circuit		At open circuit		At specified voltage	
Radiative recomb	0.00	0.00%	0.00	0.01%	0.00	0.00%
Auger recomb	0.53	1.31%	11.24	28.09%	0.56	1.40%
SHR recomb at surface	2.08	5.21%	28.74	1.86%	2.7	5.43%
SHR recomb in emitter	0.00	0.00%	0.02	0.04%	0.00	0.00%
Collected carriers	37.39	93.48%	0.00	0.00%	37.27	93.17%
Generated in emitter	40.00	100%	40.00	100%	40.00	100%

The SHR recombination at the surface is greater the SHR recombination in the emitter and the Auger recombination. And it is observed at short circuit, open circuit, and specified voltage.
The collected carriers are very important at short-circuit and at specified voltage respectively 93.48% and 93.17% while it does not exist at open circuit 0.00%/

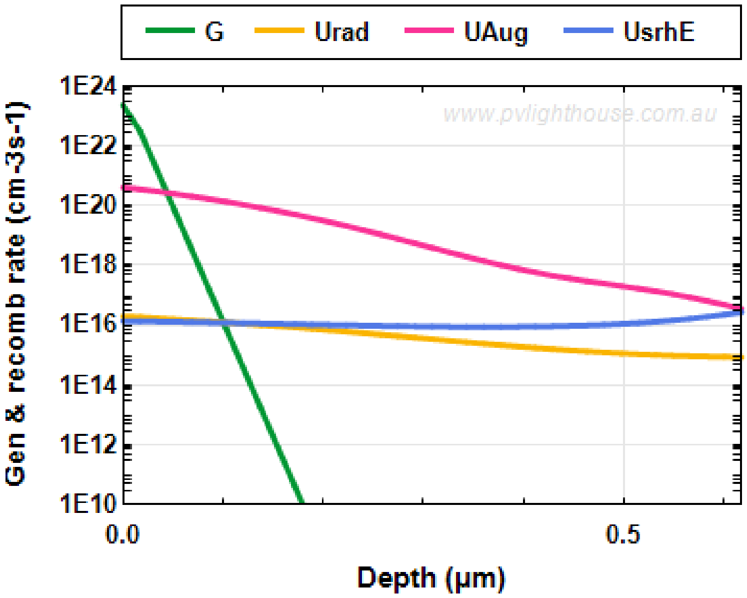

Figure 1 Recombination rates vs depth for light conditions with Vj = 0.55 V

Figure 1 shows the recombination rates on the emitter for light conditions with specified voltage value equals to 0.55 V.
The generated rate decreases exponentially and reaches 10^{10} in the vicinity of 0.18cm^{-3}/s. While the others recombination such that:
The Auger recombination rate is decreasing slowly in the emitter and changes from 10^{20} cm^{-3}/s to 10^{16} cm^{-3}/s.
The Shockley–Read–Hall (SRH) recombination is quasi constant over the 0.00um-0.5um and increases a little bite over the range 0.5um-to 0.6um.
The radiative recombination is decreasing slowly and changing from 10^{16} cm^{-3}/s to 0.8.10^{16}. cm^{-3}/s.

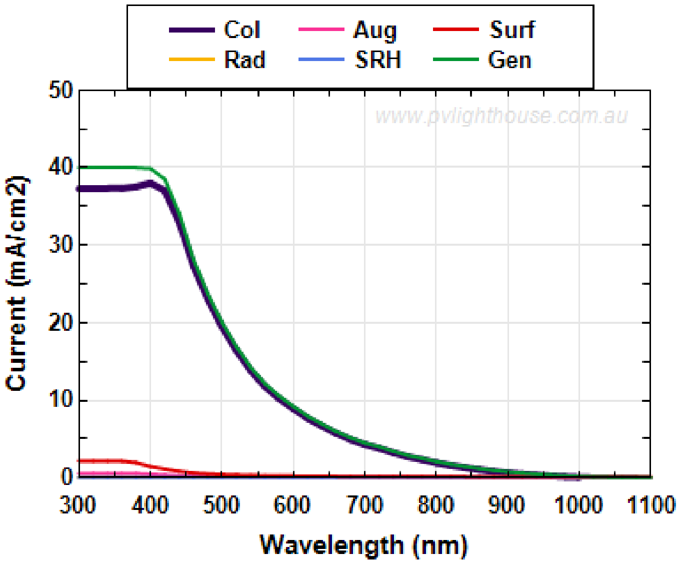

Figure 2 Current vs wavelength for light conditions

Figure 2 shows the current density at light conditions depending to the wavelengths for different types of recombination.
The current density is constant 36 mA/cm^2 for the auger recombination, the surface recombination, and the collected carriers over the range 300nm-500 nm. And it starts decreasing exponentially and reaches 0 at 1000nm.
The radiative recombination, Shockley–Read–Hall (SRH) recombination and generated current are very weak over the range 300nm-1000nm.The current does not exist for thes types of recombination.
.

CONCLUSION

In this work, the current density and the recombination rate is determined under the monochromatic illumination. The current density is verry for the Auger recombination and the surface recombination. The SHR recombination at the surface is greater the SHR recombination in the emitter and the Auger recombination. And it is observed at short circuit, open circuit, and specified voltage. And the collected carriers are important in short circuit and at specified voltage. This work could be enlarged by in dark conditions.

REFERENCE

[1] Qian wang ,Weiguo Liu, Lei Gong? Ligo Wang, Yaqing Li, Determination of doping concentration of heavily doped silicon wafers using photon reabsorption in photocarrier radiometry AIP publishing , 10, 035118 (2020)

[2] P. Auger, "Sur les rayons β secondaires produits dans un gaz par des rayons X", *C.R.A.S.*, vol. 177, pp. 169-171, 1923.

[3] G. Masetti, Severi, M., and Solmi, S., "Modeling of carrier mobility against carrier concentration in arsenic-, phosphorus-, and boron-doped silicon", IEEE Transactions on Electron Devices, vol. ED-30, pp. 764–9, 1983.

[4] Shilong Sun, Weizhong Sun, Qiuyan Hao, Lijian Wang, Xiaoyun Teng, Caichi Liu, Yuesheng XU Oxide precipitation behavior in heavily doped silicon wafer after rapid thermal process , Elsivier Material science in semiconductor processing , Volume 9, Issues 1–3, February–June 2006, Pages 78-81

[5] S. Y. Lim, S. P. Phang, T. Trupke, A. Cuevas, and D. Macdonald ; opant concentration imaging in crystalline silicon wafers by bandto-band photoluminescence; journal of applied physics ; J. Appl. Phys. 110, 113712 (2011)

[6] Dadan Hamdania,, Soni Prayogib, Yoyok Cahyonoc , Gatut Yudoyonoc , D. Darmintoc; The Effects of Dopant Concentration on the Performances of the a-SiOx:H(p)/a-Si:H(i1)/a-Si:H(i2)/μc-Si:H(n) Heterojunction Solar Cell; International Journal of Renewable Energy Development 11 (1) 2022: 173-181.

[7] J.l.B. Wilson; Is amorphous silicon played out?;Macmillan journal; Nature Vol. 295 11 February 1982

[8] R.B.M. Girisch, R.P. Mertens and R.F. De Keersmaecker, "Determination of Si-SiO2 interface recombination parameters using a gate-controlled point-junction diode under illumination," *IEEE Transactions on Electron Devices* **35**, pp. 203–22, 1988.

[9] K.R. McIntosh and P.P. Altermatt, "A freeware 1D emitter model for silicon solar cells," *Proc. 35th Photovoltiac Specialists Conference*, Honolulu, pp. 2188–2193, 2010.